Laser fluorescence experiments with a pulsed dye laser in an argon plasma

DOI:
10.1016/0022-4073(89)90121-0

Document status and date:
Published: 01/01/1989

Document Version:
Publisher’s PDF, also known as Version of Record (includes final page, issue and volume numbers)

J. Quant. Spectrosc. Radiat. Transfer Vol. 41, No. 4, pp. 251–258, 1989
Printed in Great Britain.
0022-4073/89 $3.00 + 0.00

LASER FLUORESCENCE EXPERIMENTS WITH A PULSED DYE LASER IN AN ARGON PLASMA

H. M. J. WILLEMS†, K. YUASA‡, B. VAN DER SIJDE§, D. C. SCHRAM§, and J. A. M. VAN DER MULLEN§

†NKF Kabel BV, Delft, The Netherlands, ‡Toshiba Co., Yokosuka Works, Yokosuka City, Japan and §Department of Physics, Eindhoven University of Technology, P.O. Box 513, 5600 MB Eindhoven, The Netherlands

(*Received* 14 *July* 1988)

Abstract—We have carried out laser-induced fluorescence experiments in the argon plasma of a hollow cathode arc (HCA) using a pulsed-dye laser. The pumping line was the 611.5 nm transition between the metastable $3d'\,^2G_{9/2}$ and the $4p'\,^2F_{7/2}$ level in the argon-ion system (′ refers to the ^1D core of the two times ionized argon atom). From the measured fluorescence signal of the $4p'\,^2F_{7/2}$ upper level, we are able to determine the deexcitation coefficient [$(2.5 \pm 1.0)\,10^{-14}$ m^3 sec^{-1}] and the density of the $3d'\,^2G_{9/2}$ metastable level (1.5×10^{15}–$1.25 \times 10^{16}\,\mathrm{m}^{-3}$). The $3d'\,^2G$ metastable doublet is a serious candidate for excitation of the $4p$ upper laser levels and may partly be responsible for the $4s$–$4p$ inversion which causes the argon-ion laser oscillation.

INTRODUCTION

Laser induced fluorescence (LIF) measurements can be used to get a better understanding of important elementary processes such as collisional (de)excitation in atomic systems and to determine their rate coefficients. These collisional rate coefficients provide essential input for collisional-radiative (CR) models. With these models, one can determine the excited state densities as functions of plasma parameters such as the electron density n_e and the electron temperature T_e. Especially for complicated systems such as the argon-ion system, little is known about the collisional rate coefficients. Usually, hydrogen-like formulae are used.[1,2]

The choice of the argon-ion system for our LIF measurements is based on laser action in that system. In a previous paper,[3] we presented the results of LIF measurements with a cw argon-ion laser, from which we determined the absolute value of the population inversion between $4p$ and $4s$ levels as a function of the electron density n_e.

In this paper, we report on LIF experiments performed with a pulsed-dye laser. The ultimate aim is to achieve a better understanding of the population processes of the $4p$ upper laser level, especially those originating from metastable levels.

We pumped the 611.5 nm line between the metastable $3d'\,^2G_{7/2}$ in the argon-ion system (′ refers to levels with a ^1D core, the main system has a ^3P core) of an argon plasma generated in a stationary, magnetically confined, hot, hollow-cathode arc discharge. The electron temperature is more or less constant, i.e., $T_e \approx 3.5$ eV, while the electron density was varied between 1×10^{19} and $1 \times 10^{20}\,\mathrm{m}^{-3}$. The influence of the two metastable $3d'\,^2G$ levels on the $4p$ levels may be of great importance in the quantitive explanation of the density inversion between the $4s$ doublet and the $4p$ levels. A diagram of the levels involved is shown in Fig. 1. The behaviour of the $4p'$ level, which is hereafter denoted by level a, is detected with the 461 nm line. Since the lower $3d'$ level, hereafter denoted by level b, is metastable, the density of b is substantially higher than that of a. We expect the time behaviour for the upper level indicated in Fig. 2. If the laser is switched on at time $t = 0$ the density of level a increases rapidly until saturation is reached, when the levels a and b have the same density per statistical weight. In this new situation, the common density value will decrease, mainly due to the destruction of the upper level a. The rapid increase followed by the decay is reflected by the peak in the fluorescence signal (cf. Fig. 2). The decay leads to a plateau, which reflects a steady state in which the levels a and b, coupled by the laser irradiation, share production and destruction with each other.

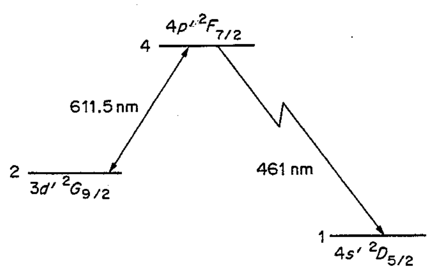

Fig. 1. A representation of the pumped transition and the fluoresence line.

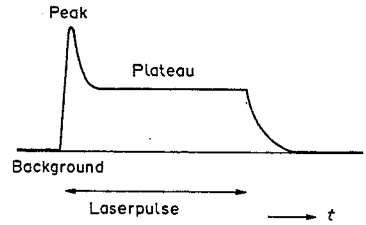

Fig. 2. The schematic time response of the fluorescence signal.

Figure 3 shows the average time behaviour of the 461 nm line, as obtained from the experiments after a number of pulses. The decay of the measured peak is spread out over 100–200 nsec, while the lifetime of the level a ($4p'$) is smaller than 10 nsec. This difference can be explained by the time resolution of 100 nsec and the jitter of the laser pulse. The experiments have shown that it is impossible to measure short decay times directly with long laser pulses. In this context, we refer to Ref. 4, where decay time mesurements in a comparable experiment in hydrogen are reported. The usual result is that the measured decay time for emission and collisions has about the same value or even a larger value than that predicted from the lifetime in spontaneous emission only.[5] We confine ourselves to the experimental results for the integrated values of the peak and the plateau and ignore the time-dependent decay structure. The observed dependency of the peak and plateau on the electron density can be explained with a simple two-level model. This comparison of measurements and theory provides information on the properties of the metastable level $3d'\,^2G_{9/2}$.

MODEL

For a proper understanding of the changes in the level densities that are induced by laser irradiation, we first consider the situation of the unperturbed plasma.

The density $n(p)$ of an excited argon-ion level p in a stationary plasma is the result of the balance between elementary production and destruction processes. This balance yields

$$n(p)\,D(p) = P(p), \tag{1}$$

in which P and D represent the production term and the destruction factor respectively.[6] In the case of an ionizing plasma the contribution to the level density [i.e., in $P(p)$] from the doubly ionized species can be neglected and we have

$$P(p) = \underbrace{n_e n_{i+} K_{+p}}_{\text{excitation from ion ground state}} + \underbrace{\sum_{1 \neq q \neq p} n_e n(q) K_{qp}}_{\text{excitation from other states}} + \underbrace{\sum_{q>p} n(q) A(q,p)}_{\text{cascade from higher states}}, \tag{2a}$$

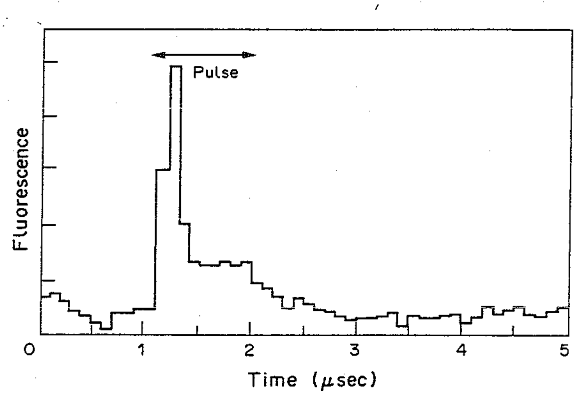

Fig. 3. An example of a fluorescence measurement (in arbitrary units) with the pulsed-dye laser.

$$D(p) = \underset{\substack{\text{collisional} \\ \text{destruction}}}{n_e K(p)} + \underset{\substack{\text{radiative} \\ \text{destruction}}}{A(p)}. \tag{2b}$$

The density of the ion ground state is denoted by n_{i+}, the total probability for radiative decay is given by

$$A(p) = \sum_{q<p} A(p, q),$$

whereas $K(p)$ is the total rate coefficient for collisional destruction including ionization. The influence of transport processes on the population density $n(p)$ is negligible since elementary processes take place on a relatively much shorter time scale. This is a normal assumption in collisional-radiative models.

An essential feature of the destruction factor of a radiative level is that it consists of an n_e-dependent and an n_e-independent part. This result implies that, for lower n_e-values, the density of a radiating level is proportional to $n_e \times n_i$ ($= n_e^2$ if $n_i = n_e$) whereas, for high n_e-values, an n_i ($= n_e$) proportionality applies. With increasing n_e at constant temperature, we expect a change in the n_e-dependence for the n_e-value given by the equality $n_e K(p) = A(p)$.

From spectroscopic measurements,[7] it is shown for the $4p$ levels in the ArII system that this change in n_e-dependence occurs for $n_e \simeq 2 \times 10^{19}\,\mathrm{m}^{-3}$. In Fig. 4, we show the absolute density of the undisturbed $4p'\,^2F_{7/2}$ level as a function of the electron density. In Fig. 4, we can construct a line with a bend at $n_e = 2 \times 10^{19}\,\mathrm{m}^{-3}$, according to Ref. 7. The lower part represents the corona model, for which $n(4p')$ is proportional to n_e^2; the upper part represents the excitation-saturation phase (ESP) for which $n(4p')$ is proportional to n_e. This picture is in accord with Ref. 7. Together with the well-known A-values,[8] we can roughly determine the destruction factor of the $4p'$ level from

$$D(p) = 1.2 \times 10^8 + 6 \times 10^{-12}\, n_e\ (\mathrm{sec}^{-1}). \tag{3}$$

For a metastable level such a change in n_e-dependence will not happen, due to the absence of the radiative part in the destruction factor. Hence, the population density of a metastable ion level scales with n_e and neither the population density nor the destruction factor can be determined by direct spectroscopic means.

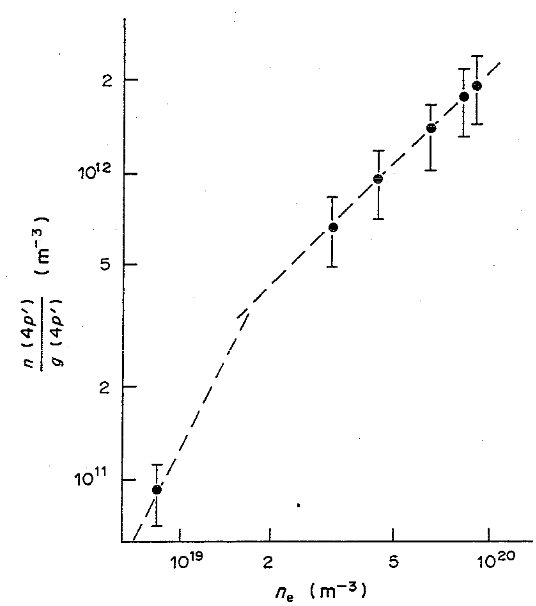

Fig. 4. The absolute density $n(4p'\,^2F_{7/2})$ per unit statistical weight of the upper level of thc fluorescence line as a function of n_e ($T_e = 3.7$ eV).

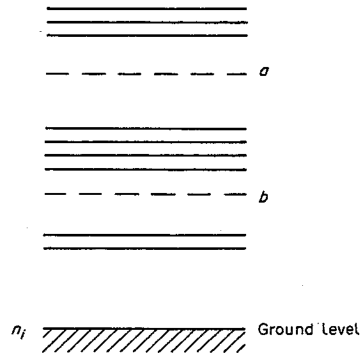

Fig. 5. A schematic representation of a simplified two-level system.

However, as the result of specific laser irradiation, the metastable level can be coupled to a radiative upper level and, under appropriate conditions, the radiation of the upper level can provide information on the destruction factor and density of the metastable level.

In a simple model, we assume that the population densities of all other levels are unaffected by the laser irradiation and that the intensity of the laser is so high that saturation is reached in a time much shorter than the lifetime of the upper level. Under this assumption, we do not need further information about the laser beam. The rates of absorption and stimulated emission supercede those of all other processes many times. As a consequence, the levels a can b can be regarded as sublevels of one level, denoted by $(a+b)$ with a total statistical weight $g(a+b) = g(a) + g(b)$ and a total density $n(a+b) = n(a) + n(b)$. For this level $(a+b)$, each state has the same density, i.e., $\tilde{\eta}(a) = \tilde{\eta}(b)$. The population density per unit statistical weight is denoted by $\eta = n/g$ and the values of quantities during the laser pulse will be marked with the $\sim$ symbol. The total density will have a time evolution which can be described by

$$\mathrm{d}\tilde{n}(a+b)/\mathrm{d}t = P^*(a) + P^*(b) - g(a)\tilde{\eta}(a)D^*(a) - g(b)\tilde{\eta}(b)D^*(b), \tag{4}$$

where $P^*(b)$ and $D^*(b)$ reflect the production and destruction of level b due to collisional-radiative interactions with all other levels except level a (cf. Fig. 5). The transitions between a and b are excluded since they do not contribute to $n(a+b)$. For the density per unit statistical weight $\tilde{\eta} \equiv \tilde{\eta}(a) = \tilde{\eta}(b)$, we obtain from Eq. (4) the following time evolution:

$$\frac{\mathrm{d}\tilde{\eta}}{\mathrm{d}t} = \frac{P^*(a) + P^*(b)}{g(a) + g(b)} - \frac{g(a)D^*(a) + g(b)D^*(b)}{g(a) + g(b)}\tilde{\eta}. \tag{5}$$

After relaxation determined by the mean depopulation factor $D^*(a+b) = [g(a)D^*(a) + g(b)D^*(b)]/[g(a) + g(b)]$, the density per unit statistical weight will tend toward

$$\tilde{\eta}_{\mathrm{plat}} = \frac{P^*(a) + P^*(b)}{g(a)D^*(a) + g(b)D^*(b)} = \frac{P^*(a) + P^*(b)}{g(a+b)D^*(a+b)}, \tag{6}$$

which is the plateau value of $\tilde{\eta}(a) = \tilde{\eta}(b)$. A measurable quantity of interest is the change in the density of level $a(=4p')$ due to the laser interaction. It is given by $\Delta n(a) = \tilde{n}(a) - n^0(a)$ and its plateau value is

$$\Delta n_{\mathrm{plat}}(a) = \frac{g(a)n^0(b) - g(b)n^0(a)}{g(a)D^*(a) + g(b)D^*(b)} D^*(b), \tag{7}$$

where $n^0(a)$ is the unperturbed density of level a. This result is obtained by using the relation $P^*(a) + P^*(b) = n^0(a)D^*(a) + n^0(b)D^*(b)$, which is valid since transitions from a to b and vice versa do not contribute to the sum of the production and destruction terms.

Another important quantity is the peak value. In our model, in which we assume that the switching time for saturation is much shorter than $D^{*-1}(a+b)$, we obtain, with $\tilde{\eta}_{\mathrm{peak}}(a) = \tilde{\eta}_{\mathrm{peak}}(b) = [n^0(a) + n^0(b)]/[(g(a) + g(b)]$,

$$\Delta n_{\mathrm{peak}}(a) = [g(a)n^0(b) - g(b)n^0(a)]/[(g(a) + g(b)]. \tag{8}$$

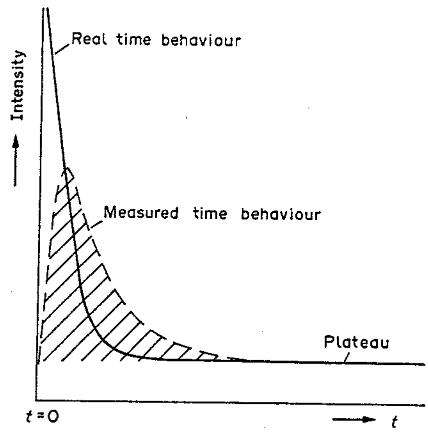

Fig. 6. A representation of the integrated peak value.

However, due to laser jitter, this peak value is not detectable in our experiments. A related measurable quantity is that of the integrated peak ΔN_{peak} (cf. the hatched area under the measured curve of Fig. 6). It can be found by integration that $\Delta N_{peak} = \Delta n_{peak}/D^*(a+b)$ so that

$$\Delta N_{peak}(a) = \frac{g(a)n^0(b) - g(b)n^0a}{[g(a)+g(b)]D^*(a+b)}. \tag{9}$$

An important quantity is the ratio of the integrated peak to that of the plateau, which is given by

$$\frac{\Delta n_{plat}(a)}{\Delta N_{peak}(a)} = \frac{[g(a)+g(b)]D^*(a+b)}{g(a)D^*(a)+g(b)D^*(b)} D^*(b) = D^*(b) = \sum_{i \neq a} K(b,i)n_e \tag{10}$$

and is found by using Eqs. (7) and (9).

A second important quantity is the ratio of the plateau to that of the background, which is given by

$$\frac{\Delta n_{plat}(a)}{n^0(a)} = \frac{g(a)n^0(b)/n^0(a) - g(b)}{g(a)D^*(a)+g(b)D^*(b)} D^*(b). \tag{11}$$

These quantities, together with the experimental results, give information regarding the metastable level.

THE EXPERIMENTAL SET-UP

The experiments have been carried out in the magnetically confined plasma of a hollow-cathode argon arc with a self-sustaining hot cathode. The experimental conditions have been chosen with a nearly constant electron temperature ($T_e \simeq 3.5$ eV), while the electron density has been varied between $n_e = 8 \times 10^{18}$ and $1 \times 10^{20}\,m^{-3}$. The n_e- and T_e-values have been determined by Thomson-scattering.[9]

In our experiments, we used a flashtube-pumped Electro Phonics Ltd model 23 dye laser. The laser has a peak output of 10 kW with a pulse duration of about 1 μsec. The laser bandwidth is 24 GHz, while the mode spacing is 136 MHz. We used Rhodamine 6G dissolved in ethanol as a dye. The repetition frequency for the laser pulses is 0.5 Hz. When we increase the pulse frequency, the reproducibility of the laser pulses deteriorates. A schematic diagram of the experimental set-up is given in Fig. 7.

The laser light is aligned through the centre of the plasma vessel and plasma column. The laser path and detection path cross each other on the axis of the plasma column. The radiation of a second line ($\lambda = 461$ nm) with the same upper level as the pumped line ($\lambda = 611.5$ nm) is observed with a 0.5-m Jarell-Ash monochromator that has a slit width of 250 μm and is equipped with a photomultiplier of the type RCA 9698 QB. The photomultiplier pulses are converted with an

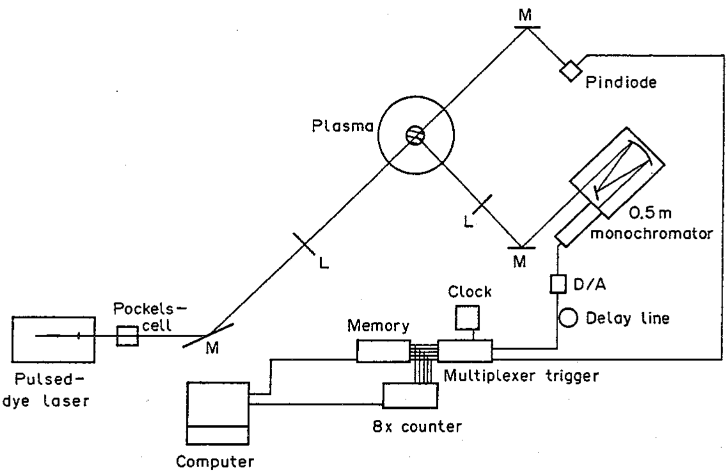

Fig. 7. A schematic lay-out of the experimental set-up; L denotes a lense, M a mirror and D/A a discriminator and an amplifier, respectively.

amplifier and discriminator into TTL-pulses. These TTL-pulses are registered with a digital recording system, which has 16 channels of 100 nsec duration. This procedure enables us to distinguish between the peak and plateau parts of the signal. The counting system is triggered by the pulses of a pin diode, which is activated by the laser pulses. The results are corrected for pile-up effects in the system by the use of Poisson statistics. We also correct for the fact that the detection volume and the plasma volume irradiated by the laser light do not match exactly.[3]

RESULTS

In Fig. 3, we present an example of a fluorescence measurement for $n_e = 4.3 \times 10^{19}\,\mathrm{m}^{-3}$. The number of photons in each channel is the accumulated result of 1000 laser shots. The signal presented is the direct result, without statistical and volume corrections. From the corrected signal, we can calculate the integrated peak value. Together with the plateau value, this approach yields a $D^*(b)$ value by using Eq. (10). In Fig. 8, we present the ratio as a function of n_e. The best fit with an n_e^{-1} dependency for high n_e-values is given with the dashed line and corresponds to a $D^*(b)/n_e = (2.5 \pm 1.0)\ 10^{-14}\,\mathrm{m}^3\ \mathrm{sec}^{-1}$. The deviation of the point at $n_e \approx 1 \times 10^{19}\,\mathrm{m}^{-3}$ is in agreement with the corona theory.

From the measured plateau and background values and the derived values of $D^*(a)$ and $D^*(b)$, we can obtain the value of $n^0(b)/n^0(a)$ by using Eq. (11), i.e., the ratio of the metastable lower level with respect to the radiative upper level. The results are given in Fig. 9 as a function of n_e. From

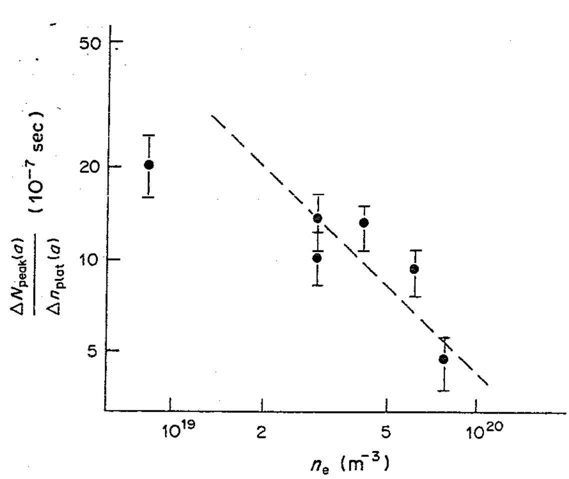

Fig. 8. The integrated peak plateau ratio $\Delta N_{peak}(a)/\Delta n_{plat}(a)$ of $4p'$ as a function of n_e.

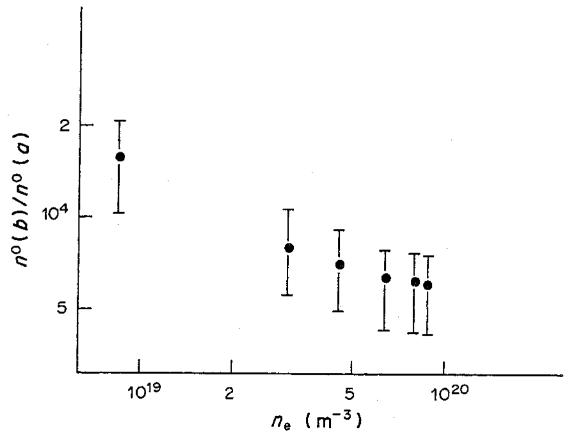

Fig. 9. The ratio $n^0(b)/n^0(a)$ of the pumped transition $3d'$ $(=b)$ and $4p'$ $(=a)$ as a function of n_e.

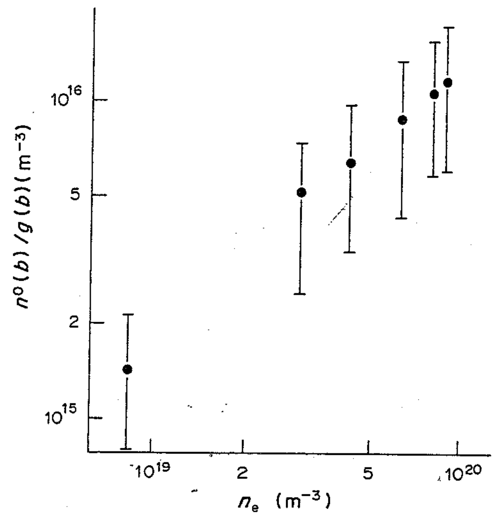

Fig. 10. The absolute density per unit statistical weight $n^0(b)/g(b)$ for the $3d'^2G_{9/2}$ level as a function of n_e.

this figure, we see that the $3d'G_{9/2}$ level is highly overpopulated with respect to the $4p'^2F_{7/2}$ level and that this ratio is nearly constant as a function of n_e and has a value of about 7×10^3. The expected deviation at $n_e = 1 \times 10^{19}$ is also demonstrated.

In Fig. 10, we show the population density of $3d'^2G_{9/2}$ per unit statistical weight as a function of n_e. These values were obtained from the results of Fig. 9 and the absolute measured densities of the $4p'$ level (see Fig. 4). This absolute density of $3d'^2G_{9/2}$ turns out to be roughly proportional to n_e, which is in agreement with the theoretical predictions and the absorption measurements of Jolly et al.[9]

DISCUSSION AND CONCLUSIONS

In our model, we assumed that the fluorescence signal is independent of the laser power, provided the latter is sufficiently great. If this condition is not fulfilled, the influence on the results will be that the measured values $\Delta n_{\text{peak}}(a)$ and $\Delta N_{\text{peak}}(a)$ are lower than for saturation and that $D^*(b)$ is lower than the calculated value.

The assumption that the population of other levels does not change significantly during the laser pulse, except for the two levels of the pumped transition, has been verified for a level that is believed to be rather sensitive to changes, namely, the $4p'^2F_{5/2}$ level, which is separated by only 0.016 eV from $4p'^2F_{7/2}$. We could not measure any change in the fluorescence signal of this level. Nevertheless, the assumption is an overall, first-order statement, since changes in the $3d'^2G_{5/2}$ and $4p'^2F_{7/2}$ populations must be demonstrated at any place in the excitation system. However, the effect is spread out over many levels so that the influence of return processes may be neglected for rough calculations.

We find a deexcitation coefficient K'_{3d} of $2.5 \times 10^{-14}\,\text{m}^3\,\text{sec}^{-1}$ for the metastable $3d'^2G_{9/2}$ level. The total deexcitation rate per unit volume and time of the $3d'^2G$ metastable doublet has been estimated to be $n_e \times n(^2G) \times K_{3d} = 5 \times 10^{19}(n_e) \times 8 \times 10^{15}[n/g(^2G) \times 18g(^2G)] \times 2.5 \times 10^{-14}(K_{3d}) = 1.5 \times 10^{23}\,\text{m}^{-3}\,\text{sec}^{-1}$.

Two possible transfer paths may be identified: back to the ground level and to other excited levels, between which the $4p$ group at an energy distance between 0.1 and 0.9 eV and a total statistical weight of 54 may be important. However, the fact that different cores are involved between the $3d'^2G$ doublet with a ^1D core and the $4p$ group (with a ^3P core) weakens this statement in favour of other $3d'$ and $4p'$ levels.

From the ratio $n(3d')/n^B(3d')$, with B denoting the Boltzmann population, which is about 0.4 for $T_e = 3.5$ eV, we can estimate that about 60% of the value of the excitation rate from the ground level is destined for excitation to other excited levels and that 40% of the excitation goes back to the ground level. Therefore, $K_{3d}^{\uparrow}$ ($\uparrow$ denotes K'_{3d} without deexcitation to the $3p$ ground level) $= 1.5 \times 10^{-14}\,\mathrm{m^3\,sec^{-1}}$ if excitation from $3d'$ to $4p'$ with an energy difference of 2.1 eV is not too large. The corresponding excitation rate is $1 \times 10^{23}\,\mathrm{m^{-3}\,sec^{-1}}$. It is of interest to compare this value with estimations for direct excitation between $3p$ and $4p$ in order to check if $3d' \to 4p$ excitation may be of importance. From Ref. 11, we find that this excitation rate is $n_e \times n_i \times K_{3p\text{–}4p} = 5\cdot10^{19} \times 5\cdot10^{19} \times 1\cdot10^{-16} \times 0.4$ (0.4 is a correction factor for model misfit, as explained in Ref. 11) $= 1 \times 10^{23}\,\mathrm{m^{-3}\,sec^{-1}}$, which is comparable with the $K_{3d}^{\uparrow}$ value. We conclude that there is a good possibility that $3d' \to 4p$ excitation contributes substantially to the $4p$ density.

Though uncertainty remains concerning the contributions of various excitation paths, we conclude that the population ratio between the metastable $3d'$ and the radiative $4p'$ levels is about 1×10^4, which is extremely high for these levels. In the case that a system is dominated by population and depopulation from collisions, which is true for $n_e > 2 \times 10^{19}\,\mathrm{m^{-3}}$, one should expect that the system is in the excitation saturation phase (ESP). The normal dependence of the population density in ESP, according to a p^{-6} relation, (p is the effective main quantum number[6]) leads to a ratio of only 4, thus being more than 3 orders smaller. Also, the population ratio of $3d'$ to the $4p$ group (19.2–20.0 eV) is possibly large, probably 80 (with densities of $8 \times 10^{15}\,\mathrm{m^{-3}}$ for $3d'$ and an estimated value of $1 \times 10^{14}\,\mathrm{m^{-3}}$ for $4p$; this last value was calculated using Ref. 11). These numbers clearly emphasize that the argon-ion system, with a number (6) of metastable levels and several extremely short-lived levels and with three different cores (^3P, ^1D, ^1S) is a very complicated system. We also conclude that laser-induced fluorescence is a promising diagnostic tool for investigating population densities and collisional transitions between excited states in plasmas.

REFERENCES

1. B. van der Sijde, J. J. A. M. van der Mullen, and D. C. Schram, *Beitr. Plasmaphys.* **24,** 447 (1984).
2. L. Vriens and A. H. M. Smeets, *Phys. Rev.* **A22,** 940 (1980).
3. K. Yuasa, H. M. J. Willems, B. van der Sijde, and D. C. Schram, *JQSRT* **40,** 135 (1988).
4. D. D. Burgess, V. P. Meyerscough, C. H. Skinner, and J. M. Ward, *J. Phys. B: Atom. Molec. Phys.* **13,** 1675 (1980).
5. D. D. Burgess, G. Kolbe, and J. M. Ward, *J. Phys. B: Atom. Molec. Phys.* **11,** 2765 (1978).
6. J. J. A. M. van der Mullen, "Excitation Equilibria in Plasmas, a Classification," Ph.D. Thesis, Eindhoven University of Technology, Eindhoven, The Netherlands (1986).
7. B. van der Sijde, B. F. M. Pots, and D. C. Schram, *J. Phys.* **40,** C7–23 (1979).
8. W. L. Wiese, M. W. Smith, and B. M. Miles, "Atomic Transition Probabilities," *NSRDS-NBS* **22,** Washington, DC (1969).
9. B. van der Sijde, S. Adema, J. C. M. de Haas, C. J. M. Denissen, and M. J. F. van de Sande, *Beitr. Plasmaphys.* **22,** 357 (1982).
10. J. Jolly, *J. Phys. Lett.* **36,** 297 (1975).
11. B. F. M. Pots, B. van der Sijde, and D. C. Schram, *Physica* **94C,** 369 (1978).